GAS Journal of Engineering and Technology (GASJET)

Volume 2 | Issue 12, 2025 Homepage: https://gaspublishers.com/gasjet-home/ ISSN: 3048-5800

Free Vibration Analysis of Rotating Composite Laminated Conical, Cylindrical Shells and Annular Plates Using Dynamic Stiffness Method

Yongguk Ri[1], Paeksan Jang[2], Songhun Kwak[3]

[1]Department of Physical Engineering, Kim Chaek University of Technology, Pyongyang 950003, Democratic People's Republic of Korea

[2]Institute of Nano- Physical Engineering, Kim Chaek University of Technology, Pyongyang 950003, Democratic People's Republic of Korea

[3]Department of Mechanical Science and Technology, Kim Chaek University of Technology, Pyongyang 950003, Democratic People's Republic of Korea

Received: *01.12.2025* | ***Accepted:*** *04.12.2025* | ***Published:*** *17.12.2025*

***Corresponding Author:** Yongguk Ri

DOI: *10.5281/zenodo.17967076*

Abstract **Original Research Article**

Free vibration of conical, cylindrical shell and annular plates with rotating composite laminates was analyzed by the dynamic stiffness method. The theoretical formulation combining the effect of the initial loop tension by the centrifugal acceleration and the Coriolis acceleration along the rotating shells was derived based on Hamilton's principle and the first-order shear deformation theory. To ensure numerical efficiency, the shell structure was divided into several segments. The state vector consists of the force compositions and displacement components of the shell segments, and the dynamic stiffness matrix for the segment was derived from the relationship between the state vector and the equations derived from it. To verify the accuracy and reliability of the proposed method, a convergence study was carried out by comparing with the results of the previous works. The results of vibration analysis for various numerical examples were presented for rotating composite laminated conical, cylindrical shell and annular plates with different rotational speeds, geometries and boundary conditions.

Keywords: Dynamic stiffness method, laminated shell, rotating shell, free vibration analysis.

1. Introduction

Rotating composite shells have been widely used in rotary systems such as high-speed centrifugal separator, advanced gas turbine and high-power aircraft jet engine because of their advantages of high strength-to-weight and stiffness-to-weight properties. In recent years, many investigations for analyzing dynamic behavior of rotating shell structures have been conducted. Dai et al. (Dai, et al., 2021) investigated damping properties of rotating laminated composite cylindrical shells based on the Love thin shell theory and Haar wavelet discretization method. Afshari (Afshari, 2020) presented a parametric study for free vibration analysis of rotating truncated conical shells reinforced with graphene nanoplatelets using generalized differential quadrature method. Shakouri (Shakouri, 2019) studied the vibration behavior of

rotating functionally graded conical shells with temperature-dependency of material properties using the Donnel shell theory. In the rotating shell, the nonlinear part of the Green-Lagrange strains is considered in order to take into account the effects of centrifugal and pressure pre-tensions, and the kinetic energy is formulated taking into account centrifugal and Coriolis terms . Nowadays, many numerical method such as Haar wavelet discretization method, semi analytical method, spectral-Tchebychev solution technique, Chebyshev–Ritz method , Fourier series solution method and finite element method are employed in the vibration study of the composite structures. Ye et al. (Ye et al., 2014) performed the free vibration analysis of open shells with arbitrary boundary conditions using a general classical shell theory in conjunction with Chebyshev polynomials and Rayleigh–Ritz procedure. Kwak et al. (Kwak et al., 2021) performed the free vibration analysis of composite laminated shells by using a newly proposed meshfree shape function. Tornabene et al. (Tornabene et al., 2014) presented the generalized differential quadrature (GDQ) method for the static and dynamic analyses of laminated doubly-curved shells and panels of revolution resting on the Winkler–Pasternak elastic foundation. Zhang et al. (Zhang et al., 2018) formulated the dynamic model of periodically coupled plate structure and truncated conical shell by using DSM.

The DSM is an exact numerical method since the dynamic stiffness of the system is obtained directly from the exact motion equations. Therefore, the DSM was employed in many studies for the dynamic analysis of different composite structures that may frequently work in a harsh environment. Liu et al. (Liu et al. 2020) proposed exact dynamic stiffness formulations for rectangular membranes and their assemblies under classical boundary conditions. An exact method for the efficient and accurate free vibration and buckling analyses of plates with general boundary conditions was built by integrating the spectral method into the classical DSM. Liu et al. (Liu et al., 2021) proposed an exact dynamic stiffness formulation for free vibration analysis of a multi-body system consisting of beam and rigid body assemblies. From the literature survey, it can be seen that the techniques for building the dynamic stiffness matrix are not the same. Banerjee and Ananthapuvirajah (Banerjee and Ananthapuvirajah, 2018) performed the free vibration analysis of functionally graded beams (FGBs) and frameworks containing FGBs by using DSM. In their study, the dynamic stiffness matrix of the FGB was formulated by applying natural boundary conditions for displacements and forces at the ends of the beam. Su and Banerjee (Su and Banerjee , 2015) formulated the dynamic stiffness matrix by relating the amplitudes of forces and displacements at the ends of the functionally graded Timoshenko beam. Li and Hua (Li and Hua, 2009) derived the dynamic stiffness matrix by directly solving the governing equations of the beam in free vibration. As an accurate and efficient modal solution technique, the Wittrick-Williams algorithm is applied to calculate the natural frequencies of the structures in DSM. El-Kaabazi and Kennedy (El-Kaabazi and Kennedy, 2012) found natural frequencies of tapered cylindrical shells using the efficient and reliable Wittrick–Williams algorithm. When use the Williams–Wittrick algorithm to determine the natural frequencies, the computing speed is very slow due to the complicated formulation of the composite shells. Therefore, Thinh and Nguyen (Thinh and Nguyen, 2013) used the adopted method to extract natural frequencies of the composite shell from the harmonic response curve. In their method, the natural frequencies of structures are corresponding to the peaks of the harmonic response curve. The computing speed of this method is faster than that of Williams–Wittrick algorithm and can reach any desired precision.

In this paper, the DSM for free vibration analysis of a rotating conical, cylindrical shells and annular plates are presented. The governing equations of the rotating shells are derived in the framework of the Hamilton's principle and the first-order shear deformation theory (FSDT). In order to take into account the effects of the initial hoop tension, the additional strain energy by the nonlinear part of the Green-Lagrange strains is considered and the kinetic energy reflecting the effects of centrifugal and Coriolis forces is formulated. The natural frequencies of the rotating laminated shells are extracted from the harmonic response curve. The

effects of parameters such as rotating speed and geometry on the free vibration of laminated conical, cylindrical shells and annular plates are investigated through some numerical examples, which may serve as benchmark data.

2. Theoretical formulations

In this section, based on the principles of FSDT and Hamilton, a governing equation for the free vibration analysis of rotating composite laminated conical, cylindrical shells and annular plates with is derived. The dynamic stiffness matrix obtained from the state vector and its derivation is applied to the free vibration analysis of rotating laminated shells.

2.1 Description of the model

The analysis model is shown in Fig.1. In laminated conical shell, length is L, semi-vertex angle is α, thickness is h small edge radius is R_1 and large edge radius is R_2. The conical shell rotates about its revolution axis in angular velocity Ω. An orthogonal curvilinear coordinate system (x, θ, z) is located on the middle surface of the shell. The symbols$\bar{U}$, $\bar{V}$, and $\bar{W}$ denote the displacements of the shell in the x, θ and z directions. The cylindrical shell and the annular plate are considered as conical shells with respectively α=0˚ and α=90˚.

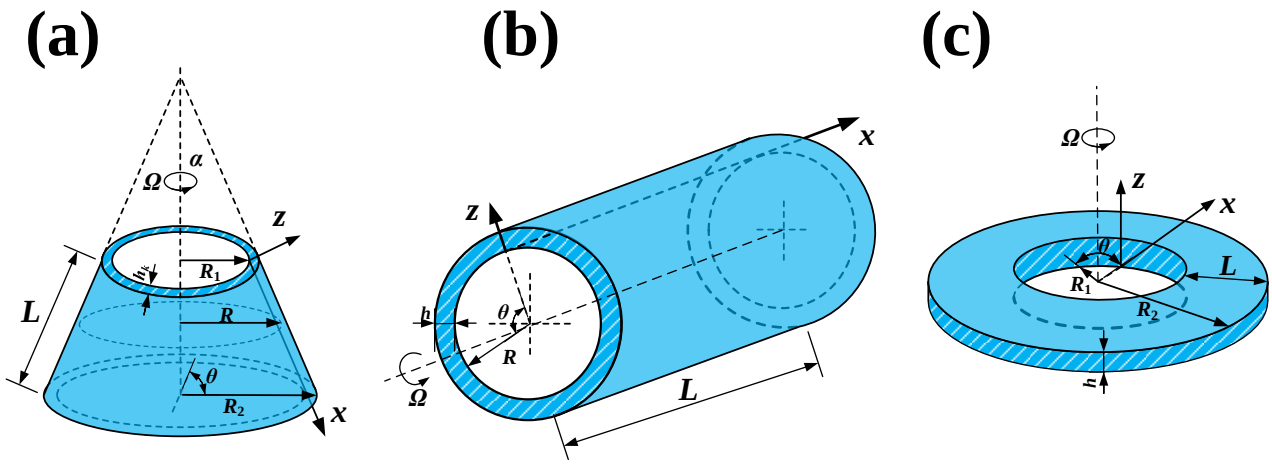

Fig. 1 Geometry of rotating laminated conical shell (a) Conical shell (b) Cylindrical shell (c) Annular plate

2.2 Governing equation and boundary conditions of the rotating laminated conical shell

According to the assumption of FSDT, the displacements of a moderately thick shell are expressed as

$$\begin{cases} \bar{U}(x,\theta,z,t) = U(x,\theta,t) + z\Psi_x(x,\theta,t) \\ \bar{V}(x,\theta,z,t) = V(x,\theta,t) + z\Psi_\theta(x,\theta,t) \\ \bar{W}(x,\theta,z,t) = W(x,\theta,t) \end{cases} \quad (1)$$

where U, V and W are the middle surface displacements of the shell in the x, θ and z directions, and Ψ_x, Ψ_θ are the rotations about θ and x axes, respectively.

The matrix form of displacement-strain relationship of the moderately thick conical shell can be expressed as

$$\boldsymbol{\varepsilon} = \boldsymbol{B}\boldsymbol{u} \quad (2)$$

where $\boldsymbol{\varepsilon}$ is a strain vector, which is composed of the middle surface strains and the curvature changes.

$$\boldsymbol{\varepsilon} = \begin{bmatrix} \varepsilon_x^0 & \varepsilon_\theta^0 & \gamma_{x\theta}^0 & \chi_x & \chi_\theta & \chi_{x\theta} & \gamma_{\theta z}^0 & \gamma_{xz}^0 \end{bmatrix}^T \tag{3}$$

where ε_i^0 and γ_{ij}^0 denote the normal and shear strains; χ_i and χ_{ij} are the curvature and twist changes. In addition, $\boldsymbol{u}$ and $\boldsymbol{B}$ represent the displacement vector and the partial differential operator matrix, respectively.

$$\boldsymbol{u} = \begin{bmatrix} U & V & W & \Psi_x & \Psi_\theta \end{bmatrix}^T \tag{4}$$

$$\boldsymbol{B} = \begin{bmatrix} \frac{\partial}{\partial x} & \frac{\sin\alpha}{R} & \frac{1}{R}\frac{\partial}{\partial\theta} & 0 & 0 & 0 & 0 & 0 \\ 0 & \frac{1}{R}\frac{\partial}{\partial\theta} & \frac{\partial}{\partial x} - \frac{\sin\alpha}{R} & 0 & 0 & 0 & -\frac{\cos\alpha}{R} & 0 \\ 0 & \frac{\cos\alpha}{R} & 0 & 0 & 0 & 0 & \frac{1}{R}\frac{\partial}{\partial\theta} & \frac{\partial}{\partial x} \\ 0 & 0 & 0 & \frac{\partial}{\partial x} & \frac{\sin\alpha}{R} & \frac{1}{R}\frac{\partial}{\partial\theta} & 0 & 1 \\ 0 & 0 & 0 & 0 & \frac{1}{R}\frac{\partial}{\partial\theta} & \frac{\partial}{\partial x} - \frac{\sin\alpha}{R} & 1 & 0 \end{bmatrix}^T \tag{5}$$

where the radius at any point R can be written as

$$R = R_1 + x\sin\alpha \tag{6}$$

Meanwhile, the matrix form of the stress resultant-strain relationship of the moderately thick conical shell can be written as

$$\boldsymbol{N} = \boldsymbol{D}\boldsymbol{\varepsilon} \tag{7}$$

where the stress resultant vector $\boldsymbol{N}$ is as

$$\boldsymbol{N} = \begin{bmatrix} \bar{N}_x & \bar{N}_\theta & \bar{N}_{x\theta} & \bar{M}_x & \bar{M}_\theta & \bar{M}_{x\theta} & \bar{Q}_\theta & \bar{Q}_x \end{bmatrix}^T \tag{8}$$

where $\bar{N}_\alpha$ and $\bar{N}_{\alpha\beta}$ indicate the normal and shear force resultants; $\bar{M}_\alpha$ and $\bar{M}_{\alpha\beta}$ are the bending and twisting moment resultants, respectively. The symbol $\bar{Q}_\alpha$ denotes the transverse shear force resultants.

In Eq. (7), the material property matrix $\boldsymbol{D}$ is given as

$$\boldsymbol{D} = \begin{bmatrix} A_{11} & A_{12} & A_{16} & B_{11} & B_{12} & B_{16} & 0 & 0 \\ A_{12} & A_{22} & A_{26} & B_{12} & B_{22} & B_{26} & 0 & 0 \\ A_{16} & A_{26} & A_{66} & B_{16} & B_{26} & B_{66} & 0 & 0 \\ B_{11} & B_{12} & B_{16} & D_{11} & D_{12} & D_{16} & 0 & 0 \\ B_{12} & B_{22} & B_{26} & D_{12} & D_{22} & D_{26} & 0 & 0 \\ B_{16} & B_{26} & B_{66} & D_{16} & D_{26} & D_{66} & 0 & 0 \\ 0 & 0 & 0 & 0 & 0 & 0 & A_{44} & A_{45} \\ 0 & 0 & 0 & 0 & 0 & 0 & A_{45} & A_{55} \end{bmatrix} \tag{9}$$

where the symbols A_{ij}, B_{ij} and D_{ij} denote the stiffness coefficients.

The strain energy of the laminated conical shell can be written as follows:

$$U = \frac{1}{2}\int_0^h \int_0^{2\pi} \int_0^L (\bar{N}_x\varepsilon_x^0 + \bar{N}_\theta\varepsilon_\theta^0 + \bar{N}_{x\theta}\gamma_{x\theta}^0 + \bar{M}_x\chi_x + \bar{M}_\theta\chi_\theta + \bar{M}_{x\theta}\chi_{x\theta} + \bar{Q}_\theta\gamma_{\theta z} + \bar{Q}_x\gamma_{xz})Rdxd\theta dz \tag{10}$$

The strain energy induced by the initial hoop tension of the rotating conical shell can be written as follows:

$$U_h = \frac{1}{2}\int_0^{2\pi}\int_0^{L} N_\theta^0 \varepsilon_\theta^{NL} R dx d\theta \tag{11}$$

where $N_\theta^0 = \rho h \Omega^2 R^2$ is the initial hoop tension caused by centrifugal force, and ρ denotes the density of the shell. The symbol ε_θ^{NL} denotes the nonlinear part of Green-Lagrange circumferential strain.

$$\begin{aligned}\varepsilon_\theta^{NL} = \frac{1}{R^2}\Bigg[&\left(\frac{\partial U}{\partial\theta}\right)^2 + \left(\frac{\partial V}{\partial\theta}\right)^2 + \left(\frac{\partial W}{\partial\theta}\right)^2 + 2\sin\alpha\left(\frac{U\partial V}{\partial\theta} - \frac{V\partial U}{\partial\theta}\right) + 2\cos\alpha\left(\frac{W\partial V}{\partial\theta} - \frac{V\partial W}{\partial\theta}\right)\\ &+ U^2\sin^2\alpha + V^2 + W^2\cos^2\alpha + 2UW\sin\alpha\cos\alpha + 2z\left(\frac{\partial U}{\partial\theta}\frac{\partial\Psi_x}{\partial\theta} + \frac{\partial V}{\partial\theta}\frac{\partial\Psi_\theta}{\partial\theta}\right)\\ &+ 2z\sin\alpha\left(\frac{U\partial\Psi_\theta}{\partial\theta} - \frac{\Psi_\theta\partial U}{\partial\theta} + \frac{\Psi_x\partial V}{\partial\theta} - \frac{V\partial\Psi_x}{\partial\theta}\right) + 2z\cos\alpha\left(\frac{W\partial\Psi_\theta}{\partial\theta} - \frac{\Psi_\theta\partial W}{\partial\theta}\right)\\ &+ 2zU\Psi_x\sin^2\alpha + 2zV\Psi_\theta + 2zW\Psi_x\sin\alpha\cos\alpha + z^2\left(\frac{\partial\Psi_x}{\partial\theta}\right)^2 + z^2\left(\frac{\partial\Psi_\theta}{\partial\theta}\right)^2\\ &+ 2z^2\sin\alpha\left(\frac{\Psi_x\partial\Psi_\theta}{\partial\theta} - \frac{\Psi_\theta\partial\Psi_x}{\partial\theta}\right) + z^2\Psi_x^2\sin^2\varphi + z^2\Psi_\theta^2\Bigg]\end{aligned} \tag{12}$$

The kinetic energy of the rotating shell can be calculated as

$$T = \frac{1}{2}\int_0^{h}\int_0^{2\pi}\int_0^{L} \rho\vec{v}\cdot\vec{v} R dx d\theta dz \tag{13}$$

where $\vec{v}$ is the absolute velocity vector.

$$\vec{v} = \dot{\vec{r}} + \Omega(-\cos\alpha\vec{i} + \sin\alpha\vec{k})\times\vec{r} \tag{14}$$

where $\vec{r} = \bar{U}\vec{i} + \bar{V}\vec{j} + \bar{W}\vec{k}$ is the displacement vector.

In the absence of external force, the set of the governing equations can be derived using Hamilton's principle.

$$\int_{t_1}^{t_2}\left(\delta T - \delta U - \delta U_h\right)dt = 0 \tag{15}$$

The obtained governing equations of the rotating conical shell are expressed as follows:

$$\begin{aligned}&\frac{\partial\bar{N}_x}{\partial x} + \frac{\sin\alpha}{R}\bar{N}_x - \frac{\sin\alpha}{R}\bar{N}_\theta + \frac{1}{R}\frac{\partial\bar{N}_{x\theta}}{\partial\theta} - I_0\frac{\partial^2 U}{\partial t^2} - I_1\frac{\partial^2\Psi_x}{\partial t^2} + 2\Omega\left(I_0\sin\alpha\frac{\partial V}{\partial t} + I_1\sin\alpha\frac{\partial\Psi_\theta}{\partial t}\right)\\ &+\Omega^2\left(I_0\frac{\partial^2 U}{\partial\theta^2} + I_1\frac{\partial^2\Psi_x}{\partial\theta^2} - 2I_0\sin\alpha\frac{\partial V}{\partial\theta} - 2I_1\sin\alpha\frac{\partial\Psi_\theta}{\partial\theta}\right) = 0\\ &\frac{1}{R}\frac{\partial\bar{N}_\theta}{\partial\theta} + \frac{\partial\bar{N}_{x\theta}}{\partial x} + 2\frac{\sin\alpha}{R}\bar{N}_{x\theta} + \frac{\cos\alpha}{R}\bar{Q}_\theta - I_0\frac{\partial^2 V}{\partial t^2} - I_1\frac{\partial^2\Psi_\theta}{\partial t^2} - 2\Omega\left(I_0\sin\alpha\frac{\partial U}{\partial t} + I_0\cos\alpha\frac{\partial W}{\partial t}\right.\\ &\left.+I_1\sin\alpha\frac{\partial\Psi_x}{\partial t}\right) + \Omega^2\left(I_0\frac{\partial^2 V}{\partial\theta^2} + I_1\frac{\partial^2\Psi_\theta}{\partial\theta^2} + 2I_0\sin\alpha\frac{\partial U}{\partial\theta} + 2I_0\cos\alpha\frac{\partial W}{\partial\theta} + 2I_1\sin\alpha\frac{\partial\Psi_x}{\partial\theta}\right) = 0\end{aligned} \tag{16}$$

$$-\frac{\cos\alpha}{R}\bar{N}_\theta+\frac{1}{R}\frac{\partial\bar{Q}_\theta}{\partial\theta}+\frac{\partial\bar{Q}_x}{\partial x}+\frac{\sin\alpha}{R}\bar{Q}_x-I_0\frac{\partial^2W}{\partial t^2}+2\Omega\left(I_0\cos\alpha\frac{\partial V}{\partial t}+I_1\cos\alpha\frac{\partial\Psi_\theta}{\partial t}\right)+$$

$$+\Omega^2\left(I_0\frac{\partial^2W}{\partial\theta^2}-2I_0\cos\alpha\frac{\partial V}{\partial\theta}-2I_1\cos\alpha\frac{\partial\Psi_\theta}{\partial\theta}\right)=0$$

$$\frac{\partial\bar{M}_x}{\partial x}+\frac{\sin\alpha}{R}\bar{M}_x-\frac{\sin\alpha}{R}\bar{M}_\theta+\frac{1}{R}\frac{\partial\bar{M}_{x\theta}}{\partial\theta}-\bar{Q}_x-I_1\frac{\partial^2U}{\partial t^2}-I_2\frac{\partial^2\Psi_x}{\partial t^2}$$

$$+2\Omega\left(I_1\sin\alpha\frac{\partial V}{\partial t}+I_2\sin\alpha\frac{\partial\Psi_\theta}{\partial t}\right)+\Omega^2\left(I_1\frac{\partial^2U}{\partial\theta^2}+I_2\frac{\partial^2\Psi_x}{\partial\theta^2}-2I_1\sin\alpha\frac{\partial V}{\partial\theta}-2I_2\sin\alpha\frac{\partial\Psi_\theta}{\partial\theta}\right)=0$$

$$\frac{1}{R}\frac{\partial\bar{M}_\theta}{\partial\theta}+\frac{\partial\bar{M}_{x\theta}}{\partial x}+2\frac{\sin\alpha}{R}\bar{M}_{x\theta}-\bar{Q}_\theta-I_1\frac{\partial^2V}{\partial t^2}-I_2\frac{\partial^2\Psi_\theta}{\partial t^2}-2\Omega\left(I_1\sin\alpha\frac{\partial U}{\partial t}+I_1\cos\alpha\frac{\partial W}{\partial t}\right.$$

$$\left.+I_2\sin\alpha\frac{\partial\Psi_x}{\partial t}\right)+\Omega^2\left(I_1\frac{\partial^2V}{\partial\theta^2}+I_2\frac{\partial^2\Psi_\theta}{\partial^2\theta}+2I_1\sin\alpha\frac{\partial U}{\partial\theta}+2I_1\cos\alpha\frac{\partial W}{\partial\theta}+2I_2\sin\alpha\frac{\partial\Psi_x}{\partial\theta}\right)=0$$

The classical boundary conditions considered in this study are as follows:

Free boundary (F): $N_x=N_\theta=Q_x=M_x=M_\theta$.

Clamped boundary (C): $u=v=w=\Psi_x=\Psi_\theta$.

Simply supported boundary (S): $u=v=w=\Psi_\theta$, $M_x=0$.

2.3 Dynamic stiffness matrix of the rotating laminated conical shell

To ensure the numerical efficiency, the conical shell is divided into N segments. For the natural symmetrical vibration mode of the ith shell segment, displacements, forces and moment resultants can be expressed as:

$$U=\sum_{n=1}^{\infty}u\cos(n\theta+\omega t)\quad V=\sum_{n=1}^{\infty}v\sin(n\theta+\omega t)\quad W=\sum_{n=1}^{\infty}w\cos(n\theta+\omega t)$$

$$\Psi_x=\sum_{n=1}^{\infty}\psi_x\cos(n\theta+\omega t)\quad \Psi_\theta=\sum_{n=1}^{\infty}\psi_\theta\sin(n\theta+\omega t)$$

$$\bar{N}_x=\sum_{n=1}^{\infty}N_x\cos(n\theta+\omega t)\quad \bar{N}_{x\theta}=\sum_{n=1}^{\infty}N_{x\theta}\sin(n\theta+\omega t)\quad \bar{M}_x=\sum_{n=1}^{\infty}M_x\cos(n\theta+\omega t)\tag{17}$$

$$\bar{M}_{x\theta}=\sum_{n=1}^{\infty}M_{x\theta}\sin(n\theta+\omega t)\quad \bar{Q}_x=\sum_{n=1}^{\infty}Q_x\cos(n\theta+\omega t)\quad \bar{N}_\theta=\sum_{n=1}^{\infty}N_\theta\cos(n\theta+\omega t)$$

$$\bar{M}_\theta=\sum_{n=1}^{\infty}M_\theta\cos(n\theta+\omega t)\quad \bar{Q}_\theta=\sum_{n=1}^{\infty}Q_\theta\sin(n\theta+\omega t)$$

where n and ω are the circumferential wave number and the natural frequency of the shell, respectively.

From Eqs. (7), (16) and (17)

$$\frac{d\boldsymbol{Y}_s}{dx}=\boldsymbol{A}_{s(10\times10)}\boldsymbol{Y}_s\tag{18}$$

where the symmetrical state vector can be written as:

$$\boldsymbol{Y}_s=\begin{bmatrix}u & v & w & \psi_x & \psi_\theta & N_x & N_{x\theta} & Q_x & M_x & M_{x\theta}\end{bmatrix}^T\tag{19}$$

The elements of matrix $\boldsymbol{A}_s$ are given in Appendix.

The symmetrical dynamic transfer matrix $\boldsymbol{T}_s$ can be expressed as follows :

$$\boldsymbol{T}_s = e^{\int_0^L \boldsymbol{A}_s dx} \tag{20}$$

$\boldsymbol{T}_s$ is then separated into four blocks.

$$\boldsymbol{T}_s = \begin{bmatrix} \boldsymbol{T}_{11} & \boldsymbol{T}_{12} \\ \boldsymbol{T}_{21} & \boldsymbol{T}_{22} \end{bmatrix} \tag{21}$$

The dynamic stiffness matrix for the symmetrical vibration of the ith shell segment is as:

$$\boldsymbol{K}_{is} = \begin{bmatrix} \boldsymbol{T}_{12}^{-1}\boldsymbol{T}_{11} & \boldsymbol{T}_{12}^{-1} \\ \boldsymbol{T}_{21} - \boldsymbol{T}_{22}\boldsymbol{T}_{12}^{-1}\boldsymbol{T}_{11} & \boldsymbol{T}_{22}\boldsymbol{T}_{12}^{-1} \end{bmatrix} = \begin{bmatrix} \boldsymbol{K}_{11}^{i} & \boldsymbol{K}_{12}^{i} \\ \boldsymbol{K}_{21}^{i} & \boldsymbol{K}_{22}^{i} \end{bmatrix} \tag{22}$$

The global symmetrical dynamic stiffness matrix for the whole conical shell is obtained by assembling the symmetrical dynamic stiffness matrices of each segment similarly as done in FEM.

$$\boldsymbol{K}_s = \begin{bmatrix} \boldsymbol{K}_{s11}^{1} & \boldsymbol{K}_{s12}^{1} & 0 & \cdots & 0 & 0 & 0 \\ \boldsymbol{K}_{s21}^{1} & \boldsymbol{K}_{s22}^{1} + \boldsymbol{K}_{s11}^{2} & \boldsymbol{K}_{s12}^{2} & \cdots & 0 & 0 & 0 \\ 0 & \boldsymbol{K}_{s21}^{2} & \boldsymbol{K}_{s22}^{2} + \boldsymbol{K}_{s11}^{3} & \cdots & 0 & 0 & 0 \\ \vdots & \vdots & \vdots & \ddots & \vdots & \vdots & \vdots \\ 0 & 0 & 0 & \cdots & \boldsymbol{K}_{s22}^{N-2} + \boldsymbol{K}_{s11}^{N-1} & \boldsymbol{K}_{12}^{N-1} & 0 \\ 0 & 0 & 0 & \cdots & \boldsymbol{K}_{s21}^{N-1} & \boldsymbol{K}_{s22}^{N-1} + \boldsymbol{K}_{s11}^{N} & \boldsymbol{K}_{s12}^{N} \\ 0 & 0 & 0 & \cdots & 0 & \boldsymbol{K}_{s21}^{N} & \boldsymbol{K}_{s22}^{N} \end{bmatrix} \tag{23}$$

Similarly, the dynamic stiffness matrix for the asymmetrical vibration $\boldsymbol{K}_a$ can be obtained. For natural asymmetrical vibration mode, the displacements, forces and moment resultants are

$$\begin{aligned} &U = \sum_{n=1}^{\infty} u \sin(n\theta + \omega t) \quad V = \sum_{n=1}^{\infty} v \cos(n\theta + \omega t) \quad W = \sum_{n=1}^{\infty} w \sin(n\theta + \omega t) \\ &\Psi_x = \sum_{n=1}^{\infty} \psi_x \sin(n\theta + \omega t) \quad \Psi_\theta = \sum_{n=1}^{\infty} \psi_\theta \cos(n\theta + \omega t) \\ &\bar{N}_x = \sum_{n=1}^{\infty} N_x \sin(n\theta + \omega t) \quad \bar{N}_{x\theta} = \sum_{n=1}^{\infty} N_{x\theta} \cos(n\theta + \omega t) \quad \bar{M}_x = \sum_{n=1}^{\infty} M_x \sin(n\theta + \omega t) \\ &\bar{M}_{x\theta} = \sum_{n=1}^{\infty} M_{x\theta} \cos(n\theta + \omega t) \quad \bar{Q}_x = \sum_{n=1}^{\infty} Q_x \sin(n\theta + \omega t) \quad \bar{N}_\theta = \sum_{n=1}^{\infty} N_\theta \sin(n\theta + \omega t) \\ &\bar{M}_\theta = \sum_{n=1}^{\infty} M_\theta \sin(n\theta + \omega t) \quad \bar{Q}_\theta = \sum_{n=1}^{\infty} Q_\theta \cos(n\theta + \omega t) \end{aligned} \tag{24}$$

Finally, the dynamic stiffness matrix of the rotating laminated conical shell is

$$\boldsymbol{K}(\omega) = \begin{bmatrix} \boldsymbol{K}_s & \boldsymbol{0} \\ \boldsymbol{0} & \boldsymbol{K}_a \end{bmatrix} \tag{25}$$

The natural frequencies of the rotating laminated conical shell can be obtained from the following condition.

$$\det\left[\boldsymbol{K}(\omega)\right] = 0 \tag{26}$$

3. Numerical results and discussions

In this section, first, the variation of dimensionless frequencies $\omega^* = \omega R_1\sqrt{\rho h/A_{11}}$ of a non-rotating composite laminated conical shell according to the number of shell segments is investigated to verify the convergence of the DSM. Next, the accuracy of the proposed method is confirmed through comparison with the results of previous literatures. Finally, numerical examples of free vibration analysis of rotating composite laminated conical, cylindrical shells and annular plates with different geometries, rotating speeds and boundary conditions are provided. The numerical results obtained by DSM are provided through self-compiled MATLAB code. Unless otherwise stated, the material properties of the shells used in the parametric study are E_2=10GPa, E_1/E_2=15, μ=0.25, G_{12}=G_{13}=6GPa, G_{23}=5GPa, and ρ=1500kg/m^2.

3.1 Verification and convergence study

To ensure the numerical efficiency, the laminated shell is divided into N segments. First, the study on the convergence of dimensionless frequencies according to the number of segments in a non-rotating cross-ply [0˚/90˚/0˚] conical shell is conducted. The small edge radius and semi-vertex angle of the conical shell are R_1=1m and α=30˚, respectively. Fig. 2 shows the variation of dimensionless frequencies with the number of segments under different boundary conditions. The circumferential and axial wave numbers of dimensionless frequency considered in Fig. 2 are n=m=1. From Fig. 2, it can be seen that the convergence characteristics of the dynamic stiffness method are independent of the type of boundary conditions and dependent on the shell geometry. In other words, the convergence characteristics of the dynamic stiffness method with segment number depend on the thickness ratio and length ratio of the laminated shell.

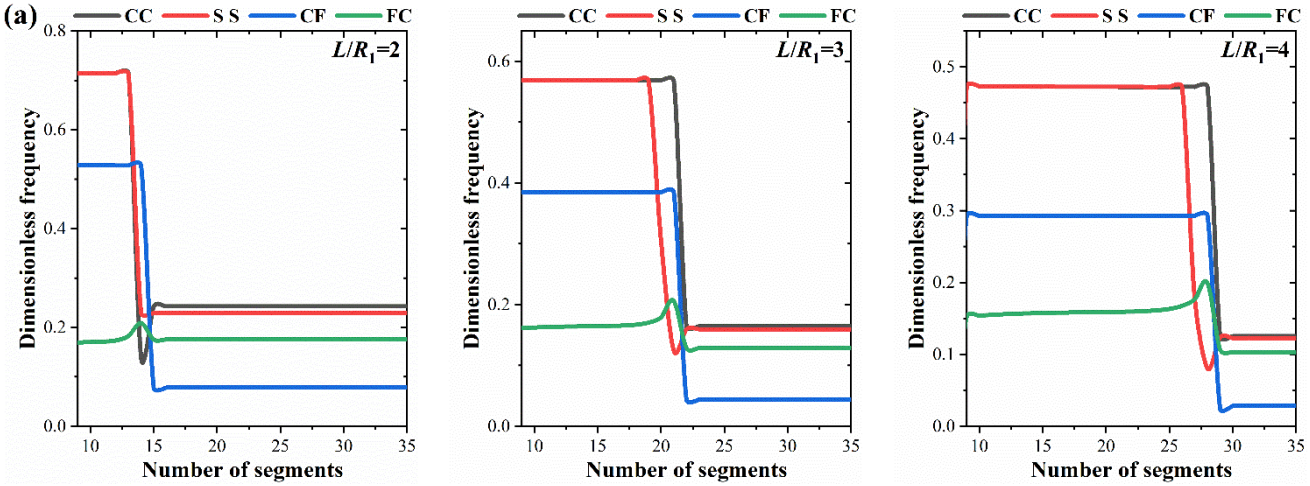

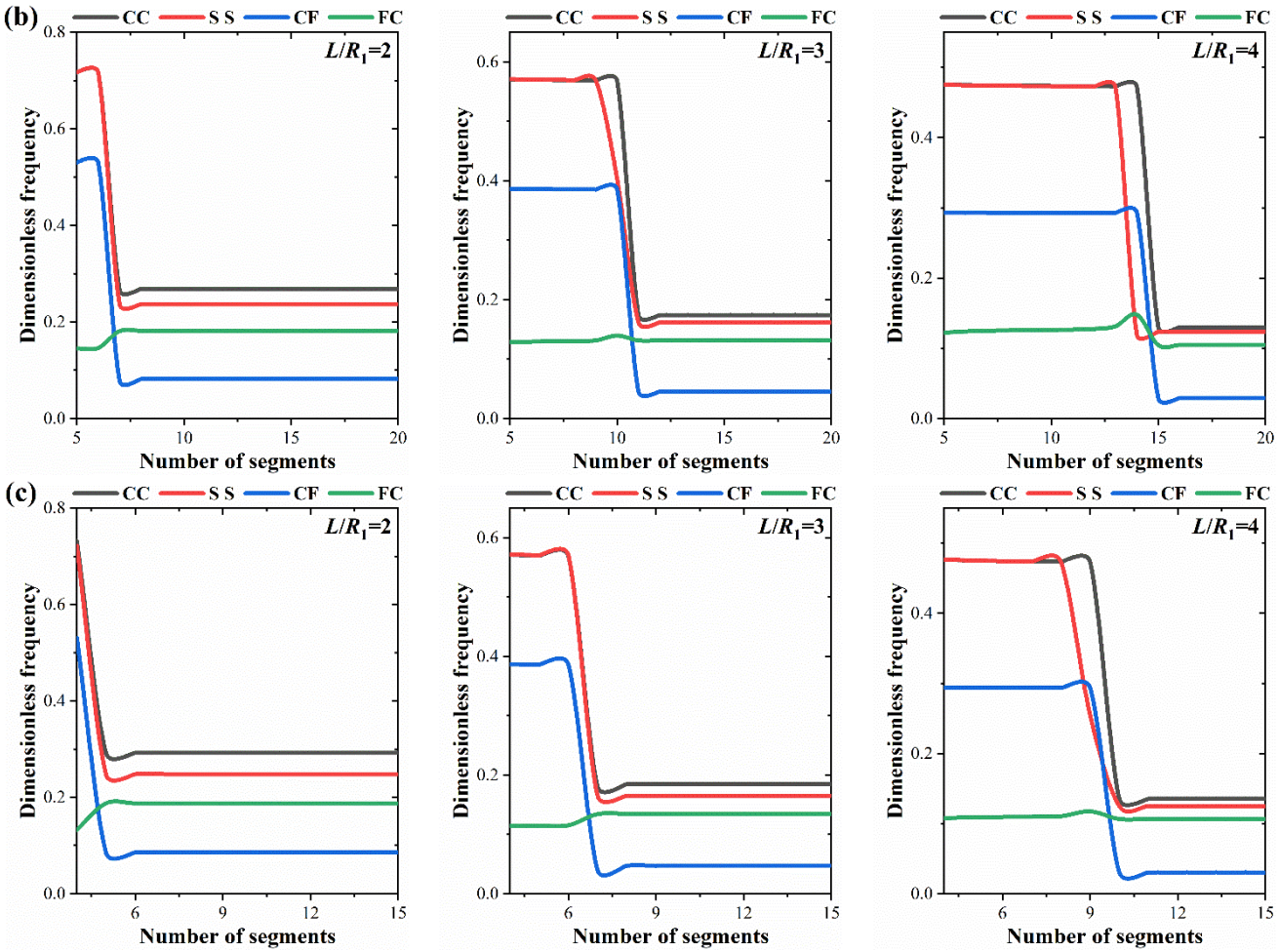

Fig. 2 Variation of the dimensionless frequencies versus the number of segments for a non-rotating laminated conical shell (a) h/R_1=0.05 (b) h/R_1=0.1 (c) h/R_1=0.15.

Subsequently, the dimensionless frequencies of composite laminated conical, cylindrical shells and annular plates obtained by DSM are compared with those of the literatures to verify the accuracy of the proposed method. In Table 1, the dimensionless frequencies of non-rotating laminated conical, cylindrical shells and annular plates with different lamination schemes and boundary conditions obtained by DSM are compared with those of the literature. In Table 2, the dimensionless frequencies $\omega^* = \omega R\sqrt{\rho(1-\mu^2)/E}$ of a rotating isotropic cylindrical shell with CC boundary condition obtained by the proposed method are compared with those of literature. In Table 3, the dimensionless frequencies $\omega^* = \omega R_2\sqrt{\rho(1-\mu^2)/E}$ of a rotating isotropic conical shell with different boundary conditions obtained by DSM are compared with those of literatures [5] and [7]. The dimensionless rotating speeds used in Tables 2 and 3 are $\Omega^* = \Omega R\sqrt{\rho(1-\mu^2)/E}$ and $\Omega^* = \Omega R_2\sqrt{\rho(1-\mu^2)/E}$, respectively. From Tables 1, 2 and 3, it can be seen that the frequency results of the laminated conical, cylindrical shells and annular plates obtained by DSM agree well with those of the literatures.

Table 1. Comparison of dimensionless frequencies for non-rotating laminated conical, cylindrical shells and annular plates (R_1=1m, L=2m, h=0.1m, n=m).

α	BCs.	n	[0/30/0]			[0/60/0]			[0/90/0]		
			Ref.	DSM	Diff, %	Ref.	DSM	Diff, %	Ref.	DSM	Diff, %
0°	CC	1	0.2980	0.2980	0.0000	0.3837	0.3837	0.0000	0.2894	0.2894	0.0000
		2	0.4564	0.4564	0.0000	0.5565	0.5565	0.0000	0.4898	0.4898	0.0000
		3	0.7000	0.6999	-0.0143	0.8044	0.8043	-0.0124	0.7601	0.7600	-0.0132
		4	0.9931	0.9930	-0.0101	1.1126	1.1124	-0.0180	1.0826	1.0824	-0.0185
	SS	1	0.2707	0.2707	0.0000	0.3621	0.3621	0.0000	0.2650	0.2650	0.0000
		2	0.3884	0.3884	0.0000	0.4939	0.4939	0.0000	0.4215	0.4214	-0.0237
		3	0.6295	0.6294	-0.0159	0.7336	0.7335	-0.0136	0.6859	0.6858	-0.0146
		4	0.9369	0.9367	-0.0213	1.0544	1.0542	-0.0190	1.0227	1.0225	-0.0196
60°	CC	1	0.1698	0.1698	0.0000	0.2128	0.2128	0.0000	0.2081	0.2081	0.0000
		2	0.3731	0.3731	0.0000	0.4205	0.4205	0.0000	0.4205	0.4205	0.0000
		3	0.6386	0.6385	-0.0157	0.7047	0.7046	-0.0142	0.7084	0.7084	0.0000
		4	0.8586	0.8589	0.0349	1.0267	1.0266	-0.0097	1.0337	1.0336	-0.0097
	SS	1	0.1110	0.1111	0.0901	0.1594	0.1595	0.0627	0.1550	0.1551	0.0645
		2	0.2884	0.2883	-0.0347	0.3322	0.3322	0.0000	0.3310	0.3310	0.0000
		3	0.5610	0.5610	0.0000	0.6218	0.6218	0.0000	0.6247	0.6246	-0.0160
		4	0.8585	0.8589	0.0466	0.9621	0.9620	-0.0104	0.9686	0.9685	-0.0103
90°	CC	1	0.1474	0.1474	0.0000	0.1611	0.1611	0.0000	0.1633	0.1633	0.0000
		2	0.3626	0.3626	0.0000	0.3960	0.3960	0.0000	0.4008	0.4007	-0.0250
		3	0.6320	0.6319	-0.0158	0.6898	0.6898	0.0000	0.6974	0.6973	-0.0143
		4	0.8253	0.8256	0.0364	1.0156	1.0155	-0.0098	1.0260	1.0259	-0.0097
	SS	1	0.0738	0.0738	0.0000	0.0808	0.0808	0.0000	0.0819	0.0819	0.0000
		2	0.2752	0.2751	-0.0363	0.3009	0.3009	0.0000	0.3046	0.3046	0.0000
		3	0.5537	0.5536	-0.0181	0.6050	0.6049	-0.0165	0.6117	0.6117	0.0000
		4	0.8253	0.8256	0.0364	0.9505	0.9503	-0.0210	0.9603	0.9602	-0.0104

Table 2. Comparison of dimensionless frequencies for a rotating isotropic cylindrical shell with CC boundary condition (L=10m, h=0.05m, m=1, μ=0.3).

n	Method	Ω*=0.0025		Ω*=0.005	
		Forward	Backward	Forward	Backward
2	Ref.	0.05991	0.05591	0.06215	0.05460
	DSM	0.06002	0.05601	0.06225	0.05424
3	Ref.	0.11455	0.11154	0.11653	0.11058
	DSM	0.11423	0.11123	0.11622	0.11020
4	Ref.	0.21314	0.21077	0.21487	0.21018
	DSM	0.23117	0.22879	0.23286	0.22811
5	Ref.	0.34226	0.34032	0.34381	0.33997
	DSM	0.33853	0.33660	0.34009	0.33622

Table 3. Comparison of dimensionless frequencies for a rotating isotropic conical shell (α=30˚, L=6m, h=0.01m, n=m=1, μ=0.3).

BCs.	Method	Ω*=0.2		Ω*=0.3	
		Forward	Backward	Forward	Backward
C-C	Ref.	0.8836	0.6018	0.9260	0.5265
	Ref.	0.8852	0.5990	0.9432	0.5198
	DSM	0.8852	0.5990	0.9432	0.5198
S-C	Ref.	0.8784	0.5963	0.9254	0.5215
	Ref.	0.8797	0.5941	0.9407	0.5160
	DSM	0.8795	0.5940	0.9406	0.5159
C-S	Ref.	0.7642	0.5357	0.8030	0.4369
	Ref.	0.7587	0.5420	0.7918	0.4504
	DSM	0.7596	0.5417	0.7927	0.4501
S-S	Ref.	0.7290	0.5331	0.7724	0.4350
	Ref.	0.7210	0.5388	0.7555	0.4479
	DSM	0.7216	0.5390	0.7560	0.4480

3.2 Parametric study

Based on the convergence and verification studies of the DSM, the parametric study for rotating composite laminated conical, cylindrical shells and annular plates with different geometries, boundary conditions, and lamination schemes is conducted in this subsection. First, the effect of the rotating speed on the dimensionless frequency of the rotating laminated shell is considered.

Fig. 3 shows the variation of the dimensionless frequency versus the rotating speed Ω in a cross-ply [0˚/90˚/0˚] conical shell with CC boundary condition. The axial wave number of dimensionless frequency considered in Fig. 3 is m=1 and the geometric parameters of the shell are R_1=1m, L=2m, h=0.1m and α=30˚. Similarly, the variation of the dimensionless frequency versus the rotating speed Ω in a cross-ply [0˚/90˚/0˚] cylindrical shell with CF boundary condition is shown in Fig. 4. The axial wave number is m=1 and the geometry of cylindrical shell is the same as in Fig. 3. As can be seen from Figs. 3 and 4, for n=0, the dimensionless frequency is not affected by the rotation direction of the shell. In addition, for n=1 and 2, the backward wave frequency decreases with the increase of the rotation speed and the forward wave frequency increase with the increase of the rotation speed. Also, the difference between the forward and backward wave frequencies increases with the increase of the rotating speed.

The effects of the semi-vertex angle on the dimensionless frequency of the rotating cross-ply [0˚/90˚/0˚] shell with different boundary conditions are illustrated in Fig. 5. The axial wave number is m=1 and the geometric parameters of the shell are R_1=1m, L=2m and h=0.1m. As seen in Fig. 5, the difference between the forward and backward wave frequencies decreases with the increase of the semi-vertex angle. In addition, the dimensionless frequency of the rotating annular plate is not affected by the rotation direction.

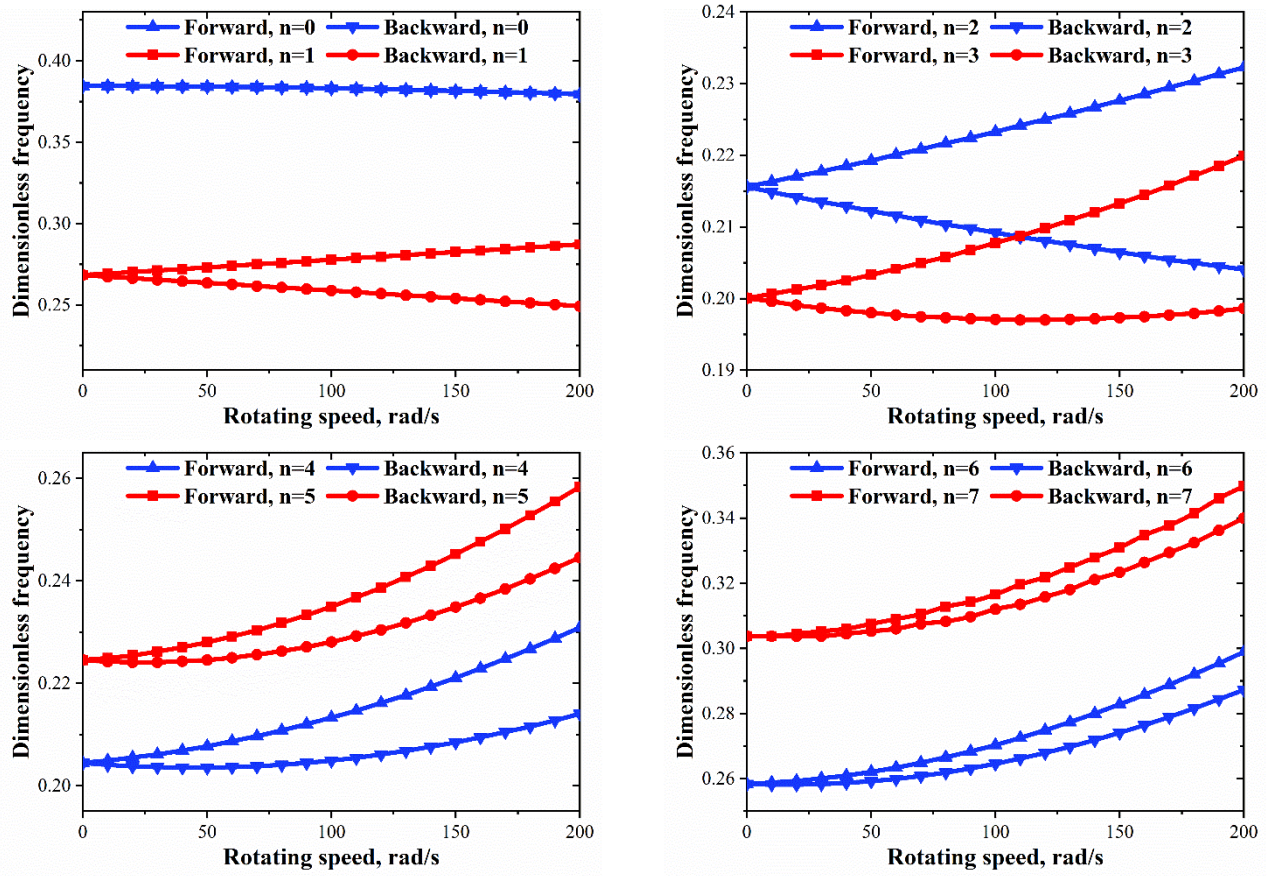

Fig. 3 Variation of the dimensionless frequencies versus the rotating speed for a laminated conical shell with CC boundary condition.

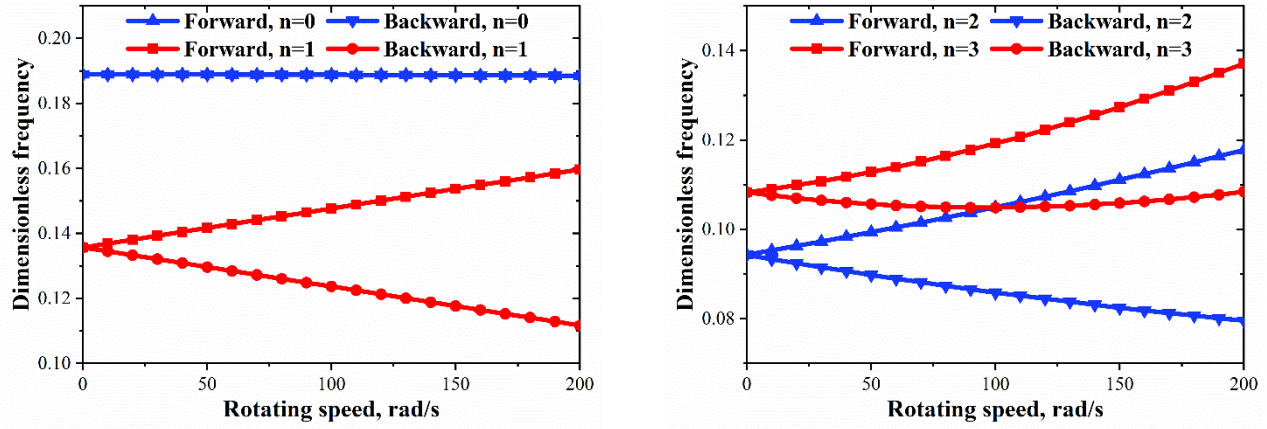

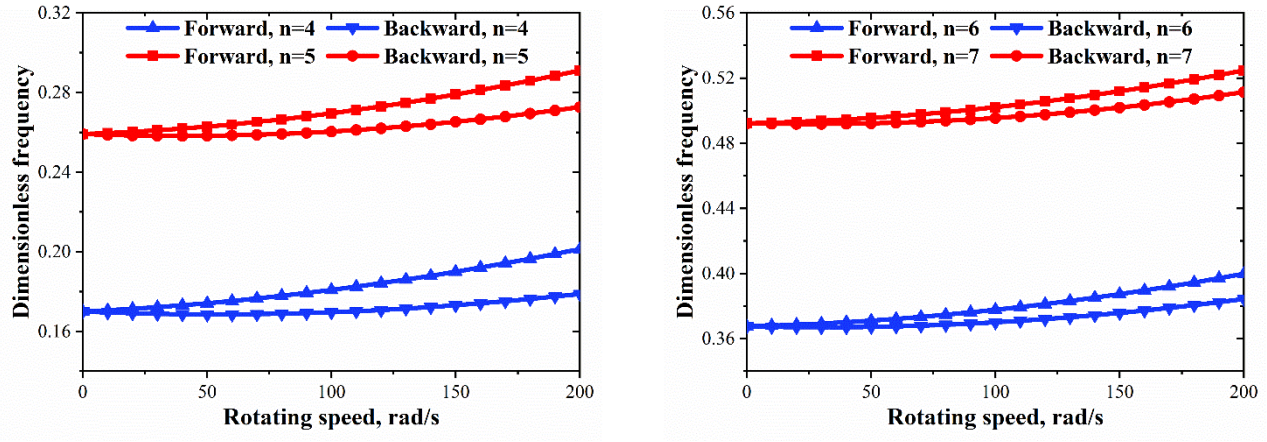

Fig. 4 Variation of the dimensionless frequencies versus the rotating speed for a laminated cylindrical shell with CF boundary condition.

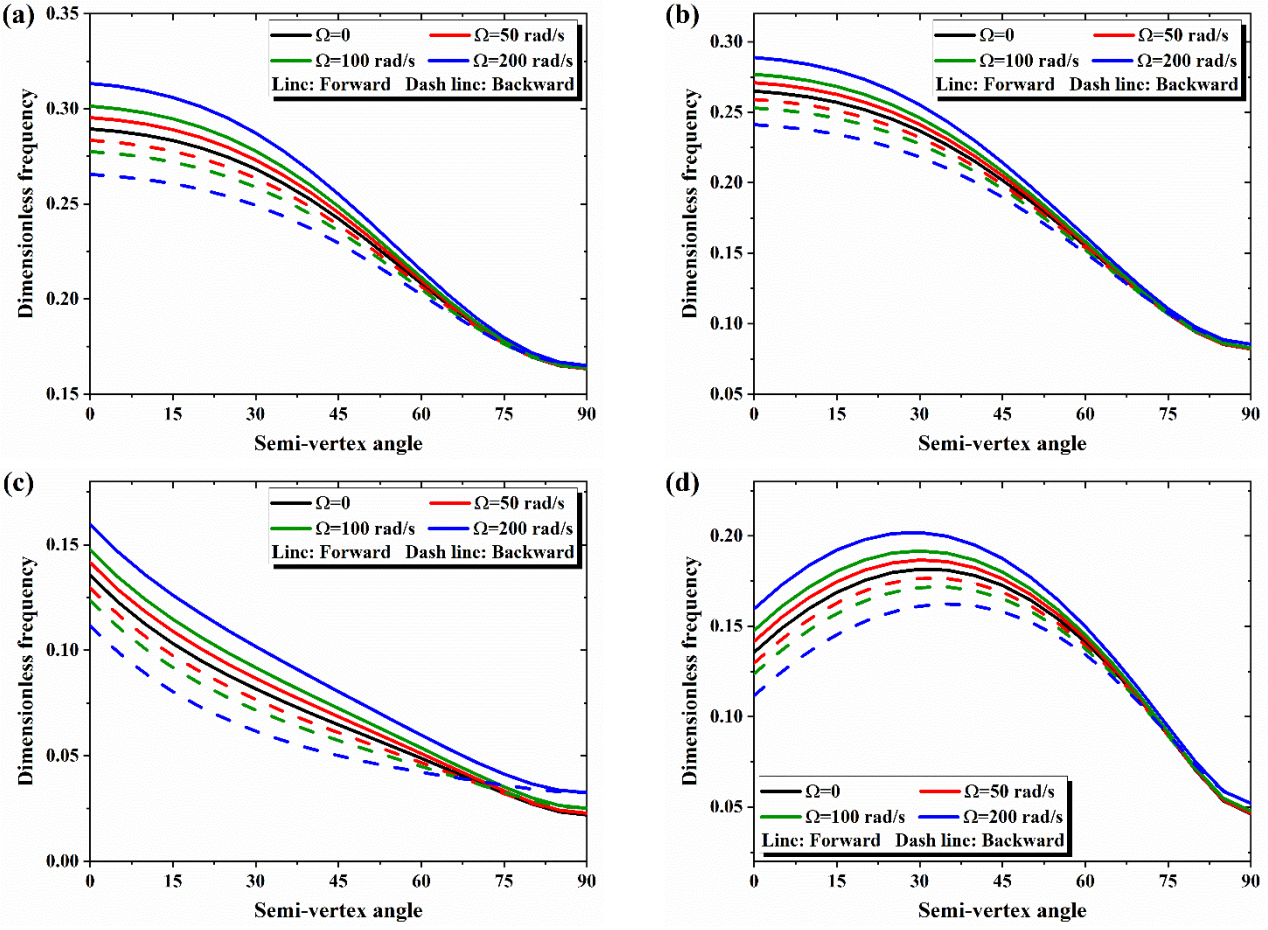

Fig. 5 Variation of the dimensionless frequencies versus the semi-vertex angle for a laminated conical shell with various rotating speed and boundary condition (a) C-C (b) S-S (c) C-F (d) F-C.

Then, the dimensionless frequencies of the rotating laminated conical shell with various boundary conditions are considered in Table 4. The mode shapes of the rotating conical shell with CC, FC and

FF boundary conditions are shown in Fig. 6. Table 5 shows the lowest four dimensionless frequencies of the rotating laminated cylindrical shell with various thicknesses and boundary conditions. As in the non-rotating shell, the frequencies in the rotating shell increase with increasing shell thickness, because the shell stiffness increases with increasing shell thickness.

Fig. 7 shows the mode shapes of rotating laminated cylindrical shell with CC and CF boundary conditions.

Finally, the dimensionless frequencies of rotating laminated annular plate with various lamination schemes and boundary conditions are shown in Table 6. As seen in Table 6, for all boundary conditions, the dimensionless frequencies decrease with the increase of length ratio L/R_1. This is because of the stiffness degradation due to the increase in the length ratio. The mode shapes of the rotating annular plate with various geometry and boundary conditions are illustrated in Fig. 8.

Table 4. Dimensionless frequencies of rotating laminated conical shell with various boundary conditions (R_1=1m, L=2m, h=0.1m, α=30˚, [0˚/90˚], Ω=50rad/s).

n	m	CC		SS		CF		FC		FF	
		Forward	Backward	Forward	Backward	Forward	Backward	Forward	Backward	Forward	Backward
1	1	0.2857	0.2747	0.2755	0.2647	0.0923	0.0810	0.2068	0.1951	0.0076	0.0053
	2	0.4997	0.4916	0.4520	0.4447	0.3458	0.3375	0.4072	0.3975	0.3106	0.3025
	3	0.7016	0.6962	0.6441	0.6386	0.5000	0.4944	0.5820	0.5752	0.4280	0.4216
2	1	0.2033	0.1948	0.1892	0.1807	0.0611	0.0527	0.1383	0.1291	0.0251	0.0175
	2	0.4023	0.3950	0.3475	0.3402	0.2454	0.2378	0.2878	0.2795	0.0495	0.0404
	3	0.6294	0.6234	0.5636	0.5576	0.4234	0.4174	0.4720	0.4650	0.3134	0.3075
3	1	0.1808	0.1739	0.1662	0.1594	0.0657	0.0592	0.1383	0.1310	0.0543	0.0482
	2	0.3639	0.3576	0.3056	0.2995	0.2052	0.1988	0.2495	0.2426	0.1126	0.1050
	3	0.5947	0.5891	0.5256	0.5200	0.3859	0.3803	0.4244	0.4182	0.2758	0.2696
4	1	0.1988	0.1929	0.1858	0.1800	0.0965	0.0910	0.1827	0.1767	0.0930	0.0877
	2	0.3656	0.3600	0.3118	0.3063	0.2127	0.2070	0.2770	0.2709	0.1815	0.1753
	3	0.5913	0.5861	0.5238	0.5187	0.3854	0.3803	0.4285	0.4228	0.2935	0.2877
5	1	0.2455	0.2403	0.2328	0.2276	0.1409	0.1361	0.2414	0.2361	0.1398	0.1350
	2	0.3989	0.3937	0.3542	0.3491	0.2556	0.2504	0.3497	0.3441	0.2481	0.2428
	3	0.6136	0.6087	0.5519	0.5469	0.4170	0.4121	0.4761	0.4708	0.3618	0.3564
6	1	0.3099	0.3050	0.2952	0.2905	0.1950	0.1905	0.3089	0.3040	0.1946	0.1902
	2	0.4584	0.4535	0.4226	0.4177	0.3201	0.3153	0.4385	0.4334	0.3186	0.3138
	3	0.6593	0.6545	0.6059	0.6012	0.4756	0.4710	0.5618	0.5566	0.4516	0.4467

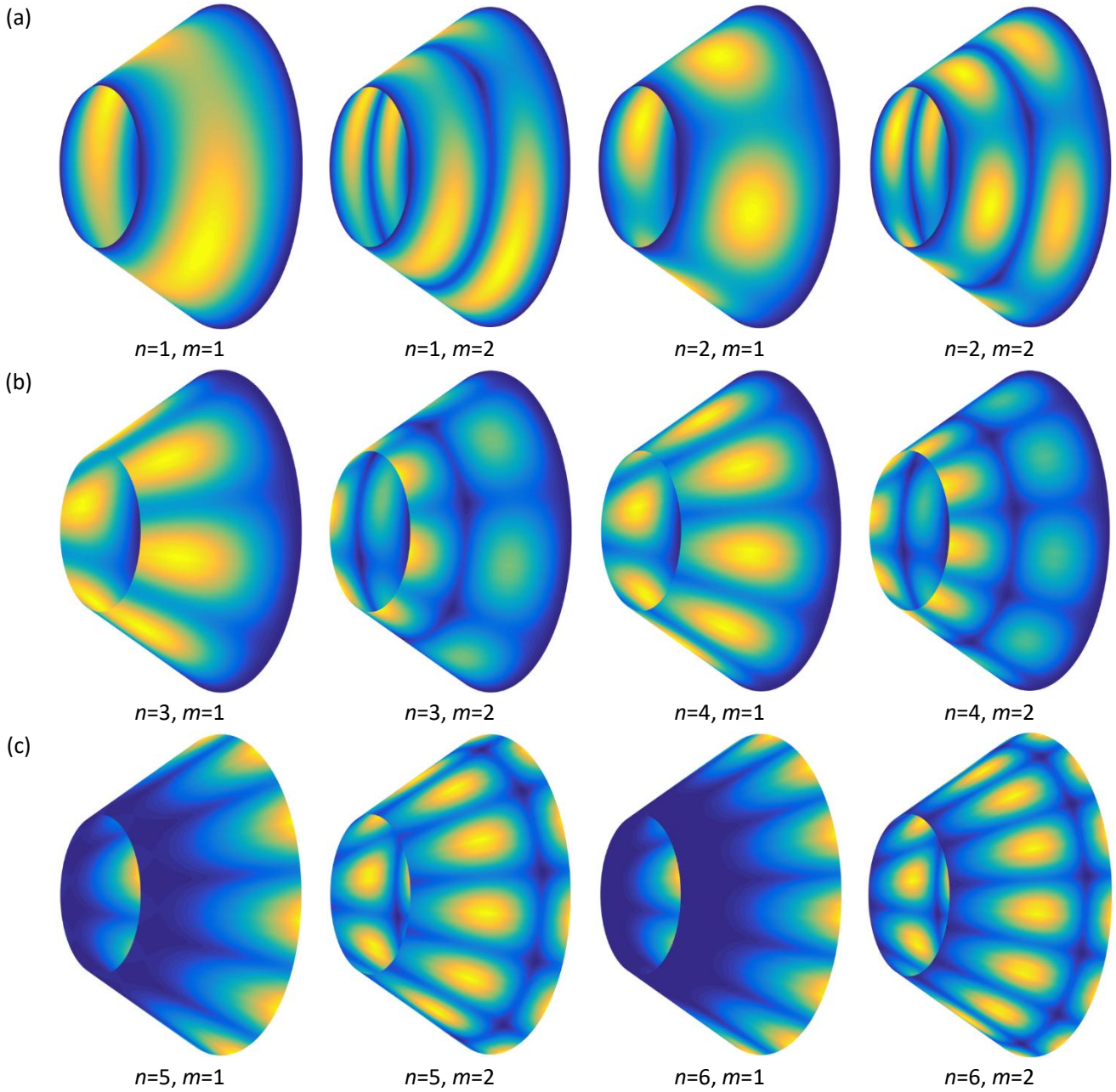

Fig. 6 Mode shapes of the rotating laminated conical shell (a) CC, Forward (b) FC, Backward (c) FF, Forward.

Table 5. Dimensionless frequencies of the rotating laminated cylindrical shell with various thicknesses and boundary conditions (R=1m, L=4m, [0˚/90˚], Ω=50rad/s).

h/R	ω^*	[0/90]				[0/90/0]			
		CC		CF		CC		CF	
		Forward	Backward	Forward	Backward	Forward	Backward	Forward	Backward
0.02	1	0.0745	0.0661	0.0424	0.0314	0.0610	0.0553	0.0327	0.0255
	2	0.0781	0.0713	0.0424	0.0340	0.0653	0.0582	0.0386	0.0290
	3	0.0980	0.0871	0.0641	0.0574	0.0709	0.0663	0.0434	0.0378

	4	0.1024	0.0967	0.0749	0.0613	0.0882	0.0786	0.0621	0.0575
0.05	1	0.0974	0.0887	0.0490	0.0379	0.0816	0.0744	0.0419	0.0323
	2	0.1018	0.0908	0.0746	0.0610	0.0933	0.0838	0.0525	0.0453
	3	0.1235	0.1162	0.0773	0.0686	0.1014	0.0957	0.0679	0.0560
	4	0.1557	0.1420	0.1073	0.1073	0.1400	0.1280	0.0873	0.0817
0.1	1	0.1133	0.1021	0.0662	0.0549	0.1055	0.0960	0.0512	0.0416
	2	0.1560	0.1424	0.0742	0.0606	0.1192	0.1120	0.0687	0.0567
	3	0.1577	0.1486	0.1073	0.1073	0.1439	0.1319	0.0916	0.0844
	4	0.2057	0.1946	0.1344	0.1233	0.1781	0.1725	0.0944	0.0944
0.15	1	0.1284	0.1170	0.0738	0.0603	0.1203	0.1107	0.0631	0.0535
	2	0.1567	0.1430	0.0854	0.0740	0.1483	0.1363	0.0694	0.0575
	3	0.2133	0.2037	0.1073	0.1073	0.1594	0.1522	0.0944	0.0944
	4	0.2146	0.2146	0.1484	0.1373	0.1889	0.1889	0.1304	0.1233

(a)

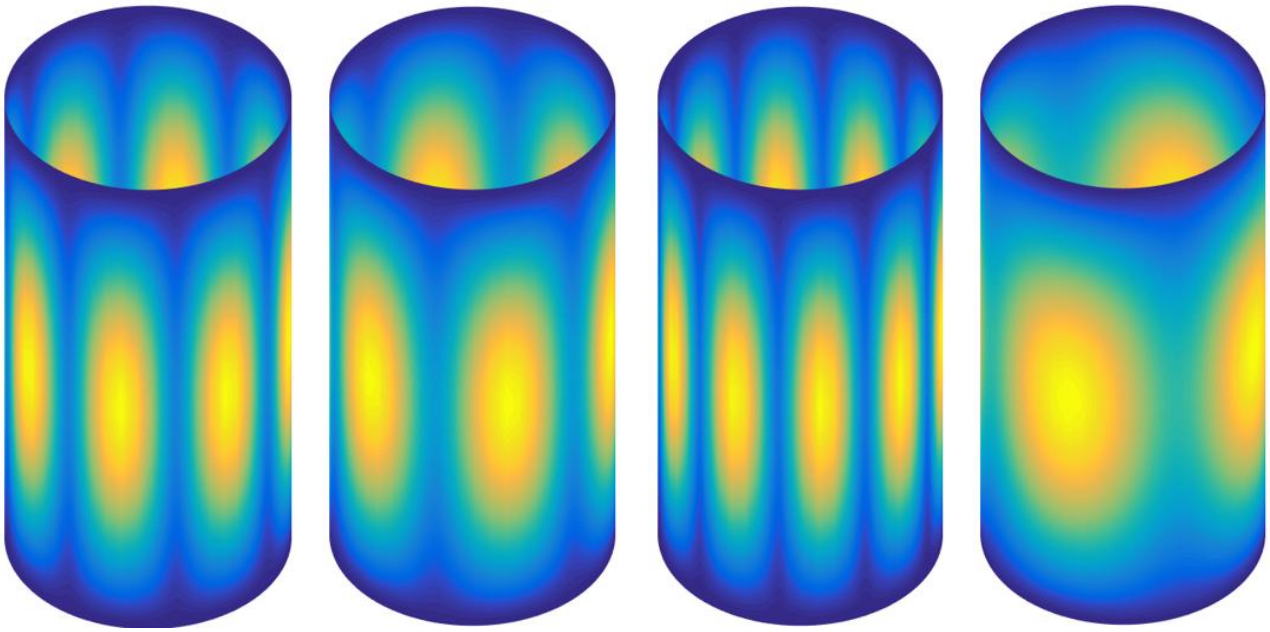

1st mode 2nd mode 3rd mode 4th mode

(b)

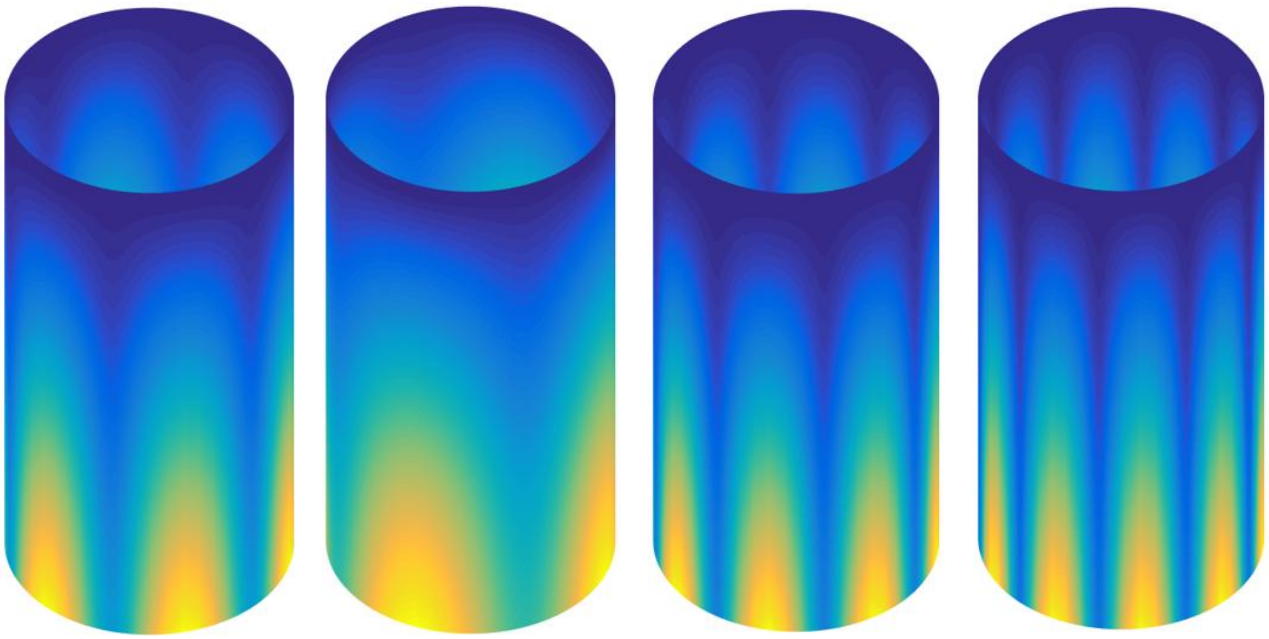

Fig. 7 Mode shapes of the rotating laminated cylindrical shell (h/R_1=0.02, [0˚/90˚/0˚]) (a) CC, Forward (b) CF, Forward

Table 6. Dimensionless frequencies of the rotating laminated annular plate with various lamination schemes and boundary conditions (R_1=1m, h=0.1m, m=n, Ω=50rad/s).

L/R_1	n	[0/90]			[0/90/0]			[0/90/0/90]		
		CC	CS	CF	CC	CS	CF	CC	CS	CF
0.5	1	1.1210	0.9223	0.2419	1.2262	1.0486	0.3531	1.2702	1.0456	0.3087
	2	2.2892	2.1848	1.1409	1.9273	1.9273	1.2243	2.3417	2.3382	1.3780
	3	2.8868	2.8848	2.1600	2.4649	2.4327	1.7100	2.9270	2.9269	2.1949
1	1	0.3732	0.2816	0.0622	0.5011	0.3818	0.0939	0.4671	0.3439	0.0801
	2	0.8937	0.7825	0.3688	1.0784	1.0087	0.5218	1.0672	0.9609	0.4746
	3	1.5400	1.4348	0.9398	1.6339	1.6339	1.1883	1.7801	1.7026	1.1641
1.5	1	0.1811	0.1320	0.0279	0.2675	0.1904	0.0409	0.2347	0.1643	0.0355
	2	0.4583	0.3894	0.1768	0.6208	0.5539	0.2652	0.5782	0.4986	0.2323
	3	0.8282	0.7522	0.4756	1.0434	0.9939	0.6725	1.0122	0.9389	0.6132
2	1	0.1061	0.0762	0.0165	0.1634	0.1118	0.0228	0.1392	0.0950	0.0205
	2	0.2757	0.2310	0.1039	0.4010	0.3461	0.1580	0.3582	0.3014	0.1370
	3	0.5130	0.4598	0.2867	0.6977	0.6495	0.4233	0.6504	0.5909	0.3765
2.5	1	0.0695	0.0495	0.0116	0.1091	0.0729	0.0149	0.0915	0.0617	0.0139
	2	0.1834	0.1525	0.0688	0.2781	0.2349	0.1042	0.2419	0.2009	0.0906
	3	0.3477	0.3094	0.1922	0.4979	0.4552	0.2891	0.4509	0.4043	0.2547
3	1	0.0493	0.0349	0.0094	0.0777	0.0511	0.0110	0.0647	0.0434	0.0107
	2	0.1308	0.1084	0.0498	0.2031	0.1691	0.0739	0.1740	0.1435	0.0649
	3	0.2514	0.2231	0.1392	0.3718	0.3353	0.2094	0.3305	0.2940	0.1847

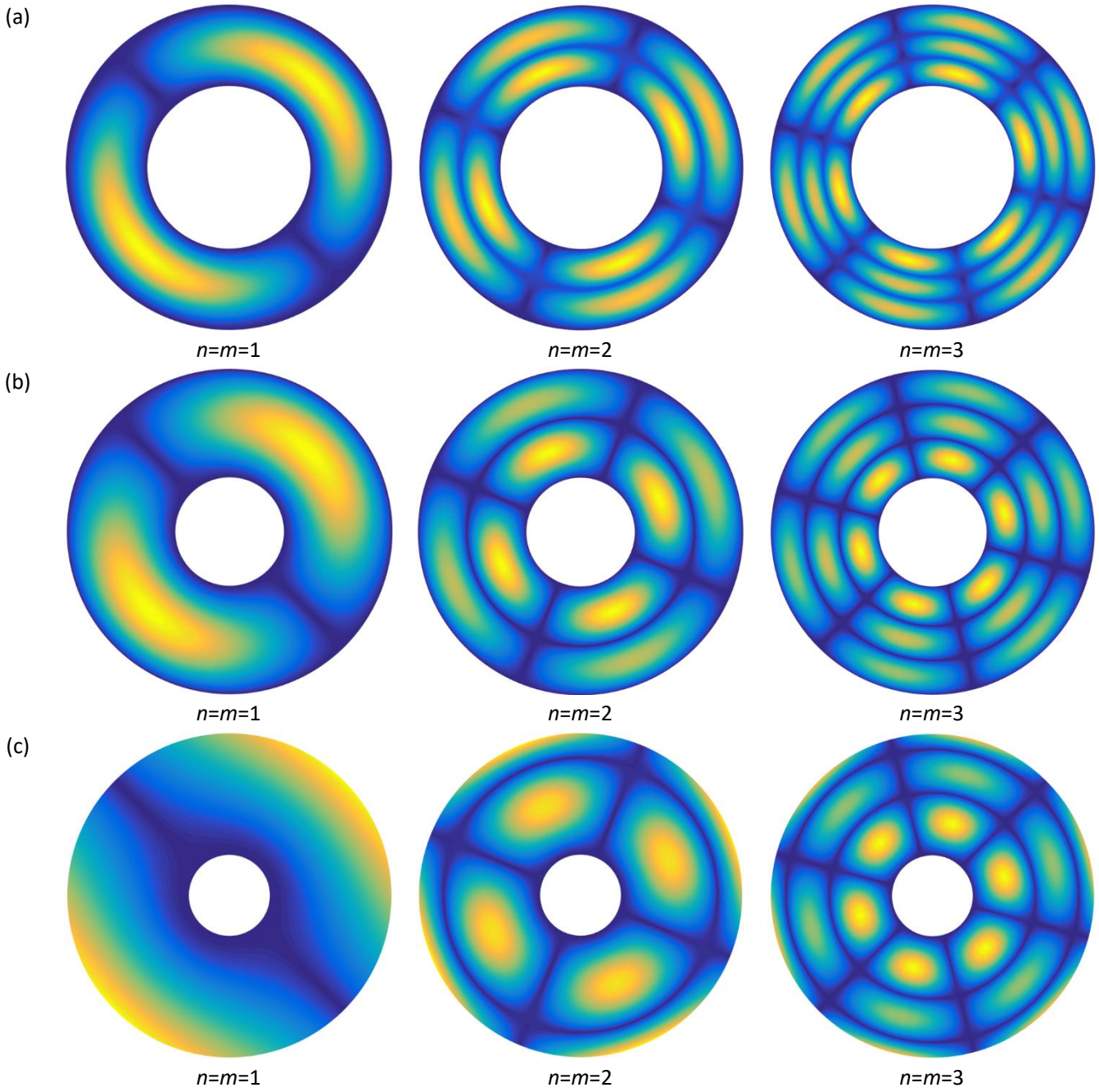

Fig. 8 Mode shapes of rotating laminated annular plate (a) L/R_1=1, CC, [0˚/90˚] (b) L/R_1=2, CS, [0˚/90˚/0˚] (c) L/R_1=3, CF, [0˚/90˚/0˚/90˚].

4. Conclusions

In this study, free vibration analysis of rotating composite laminated conical, cylindrical shells and annular plates is carried out using DSM. The governing equations of the rotating laminated shells are obtained using Hamilton's principle and FSDT. The effects of initial loop tension on the centrifugal and Coriolis accelerations are considered by introducing a nonlinear part of the Green-Lagrange strain. The shell structure is divided into several segments and the dynamic stiffness matrix for each segment is derived from the state vector and its

derivation relations. The dynamic stiffness matrix for the entire shell structure is established by assembling the dynamic stiffness matrix for each shell segment by the compatibility condition of the displacement. The convergence of the natural frequency with the number of segments is investigated and the accuracy of the proposed method is verified by comparison with the results of the published paper. Finally, the results of free vibration analysis of a cone, cylindrical shell and annular plate with rotating composite laminates with different rotational speeds, geometries and boundary conditions are presented.

Acknowledgment

I would like to take the opportunity to express my hearted gratitude to all those who make a contribution to the completion of my article.

Conflict of interest

The authors declare that there is no conflict of interest regarding the publication of this paper.

Disclosure statement

No potential conflict of interest was reported by the authors.

Data Availability

The data that support the findings of this study are available within the article.

Appendix

$$A_{s0101}=\frac{A_{12}D_{11}-B_{11}B_{12}}{B_{11}^2-A_{11}D_{11}}\frac{\sin\alpha}{R}\quad A_{s0102}=\frac{A_{12}D_{11}-B_{11}B_{12}}{B_{11}^2-A_{11}D_{11}}\frac{n}{R}\quad A_{s0103}=\frac{A_{12}D_{11}-B_{11}B_{12}}{B_{11}^2-A_{11}D_{11}}\frac{\cos\alpha}{R}$$

$$A_{s0104}=\frac{B_{12}D_{11}-B_{11}D_{12}}{B_{11}^2-A_{11}D_{11}}\frac{\sin\alpha}{R}\quad A_{s0105}=\frac{B_{12}D_{11}-B_{11}D_{12}}{B_{11}^2-A_{11}D_{11}}\frac{n}{R}\quad A_{s0106}=-\frac{D_{11}}{B_{11}^2-A_{11}D_{11}}\quad A_{s0107}=0$$

$$A_{s0108}=0\quad A_{s0109}=\frac{B_{11}}{B_{11}^2-A_{11}D_{11}}\quad A_{s0110}=0$$

$$A_{s0201}=\frac{n}{R}\quad A_{s0202}=\frac{\sin\alpha}{R}\quad A_{s0203}=0\quad A_{s0204}=0\quad A_{s0205}=0$$

$$A_{s0206}=0\quad A_{s0207}=-\frac{D_{66}}{B_{66}^2-A_{66}D_{66}}\quad A_{s0208}=0\quad A_{s0209}=0\quad A_{s0210}=\frac{B_{66}}{B_{66}^2-A_{66}D_{66}}$$

$$A_{s0301}=0\quad A_{s0302}=0\quad A_{s0303}=0\quad A_{s0304}=-1\quad A_{s0305}=0$$

$$A_{s0306}=0\quad A_{s0307}=0\quad A_{s0308}=\frac{1}{A_{55}}\quad A_{s0309}=0\quad A_{s0310}=0$$

$$A_{s0401}=\frac{A_{12}B_{11}-A_{11}B_{12}}{A_{11}D_{11}-B_{11}^2}\frac{\sin\alpha}{R}\quad A_{s0402}=\frac{A_{12}B_{11}-A_{11}B_{12}}{A_{11}D_{11}-B_{11}^2}\frac{n}{R}\quad A_{s0403}=\frac{A_{12}B_{11}-A_{11}B_{12}}{A_{11}D_{11}-B_{11}^2}\frac{\cos\alpha}{R}$$

$$A_{s0404}=\frac{B_{11}B_{12}-A_{11}D_{12}}{A_{11}D_{11}-B_{11}^2}\frac{\sin\alpha}{R}\quad A_{s0405}=\frac{B_{11}B_{12}-A_{11}D_{12}}{A_{11}D_{11}-B_{11}^2}\frac{n}{R}\quad A_{s0406}=-\frac{B_{11}}{A_{11}D_{11}-B_{11}^2}\quad A_{s0407}=0$$

$$A_{s0408}=0\quad A_{s0409}=\frac{A_{11}}{A_{11}D_{11}-B_{11}^2}\quad A_{s0410}=0$$

$$A_{s0501}=0 \quad A_{s0502}=0 \quad A_{s0503}=0 \quad A_{s0504}=\frac{n}{R} \quad A_{s0505}=\frac{\sin\alpha}{R}$$

$$A_{s0506}=0 \quad A_{s0507}=-\frac{B_{66}}{A_{66}D_{66}-B_{66}^2} \quad A_{s0508}=0 \quad A_{s0509}=0 \quad A_{s0510}=\frac{A_{66}}{A_{66}D_{66}-B_{66}^2}$$

$$A_{s0601}=\left[\left(\frac{A_{12}^2D_{11}+A_{11}B_{12}^2-2A_{12}B_{11}B_{12}}{B_{11}^2-A_{11}D_{11}}+A_{22}\right)\frac{\sin^2\alpha}{R^2}-I_0\omega^2+I_0\Omega^2n^2\right]$$

$$A_{s0602}=\left(\frac{A_{12}^2D_{11}+A_{11}B_{12}^2-2A_{12}B_{11}B_{12}}{B_{11}^2-A_{11}D_{11}}+A_{22}\right)\frac{n\sin\alpha}{R^2}+2I_0\sin\alpha(\Omega^2n-\Omega\omega)$$

$$A_{s0603}=\left(\frac{A_{12}^2D_{11}+A_{11}B_{12}^2-2A_{12}B_{11}B_{12}}{B_{11}^2-A_{11}D_{11}}+A_{22}\right)\frac{\sin\alpha\cos\alpha}{R^2}$$

$$A_{s0604}=\left[\left(\frac{A_{12}B_{12}D_{11}+A_{11}B_{12}D_{12}-A_{12}B_{11}D_{12}-B_{11}B_{12}^2}{B_{11}^2-A_{11}D_{11}}+B_{22}\right)\frac{\sin^2\alpha}{R^2}-I_1\omega^2+I_1\Omega^2n^2\right]$$

$$A_{s0605}=\left(\frac{A_{12}B_{12}D_{11}+A_{11}B_{12}D_{12}-A_{12}B_{11}D_{12}-B_{11}B_{12}^2}{B_{11}^2-A_{11}D_{11}}+B_{22}\right)\frac{n\sin\alpha}{R^2}+2I_1\sin\alpha(\Omega^2n-\Omega\omega)$$

$$A_{s0606}=\left(\frac{B_{11}B_{12}-A_{12}D_{11}}{B_{11}^2-A_{11}D_{11}}-1\right)\frac{\sin\alpha}{R} \quad A_{s0607}=-\frac{n}{R}$$

$$A_{s0608}=0 \quad A_{s0609}=\frac{\sin\alpha(A_{12}B_{11}-A_{11}B_{12})}{R(B_{11}^2-A_{11}D_{11})} \quad A_{s0610}=0$$

$$A_{s0701}=\left(\frac{A_{12}^2D_{11}+A_{11}B_{12}^2-2A_{12}B_{11}B_{12}}{B_{11}^2-A_{11}D_{11}}+A_{22}\right)\frac{n\sin\alpha}{R^2}+2I_0\sin\alpha(\Omega^2n-\Omega\omega)$$

$$A_{s0702}=\left[\left(\frac{A_{12}^2D_{11}+A_{11}B_{12}^2-2A_{12}B_{11}B_{12}}{B_{11}^2-A_{11}D_{11}}+A_{22}\right)\frac{n^2}{R^2}+A_{44}\frac{\cos^2\alpha}{R^2}-I_0\omega^2+I_0\Omega^2n^2\right]$$

$$A_{s0703}=\left(\frac{A_{12}^2D_{11}+A_{11}B_{12}^2-2A_{12}B_{11}B_{12}}{B_{11}^2-A_{11}D_{11}}+A_{22}+A_{44}\right)\frac{n\cos\alpha}{R^2}+2I_0\cos\alpha(\Omega^2n-\Omega\omega)$$

$$A_{s0704}=\left(\frac{A_{12}B_{12}D_{11}+A_{11}B_{12}D_{12}-A_{12}B_{11}D_{12}-B_{11}B_{12}^2}{B_{11}^2-A_{11}D_{11}}+B_{22}\right)\frac{n\sin\alpha}{R^2}+2I_1\sin\alpha(\Omega^2n-\Omega\omega)$$

$$A_{s0705}=\left[\left(\frac{A_{12}B_{12}D_{11}+A_{11}B_{12}D_{12}-A_{12}B_{11}D_{12}-B_{11}B_{12}^2}{B_{11}^2-A_{11}D_{11}}+B_{22}\right)\frac{n^2}{R^2}-A_{44}\frac{\cos\alpha}{R}-I_1\omega^2+I_1\Omega^2n^2\right]$$

$$A_{s0706}=\frac{n(B_{11}B_{12}-A_{12}D_{11})}{R(B_{11}^2-A_{11}D_{11})} \quad A_{s0707}=-2\frac{\sin\alpha}{R} \quad A_{s0708}=0 \quad A_{s0709}=\frac{n(A_{12}B_{11}-A_{11}B_{12})}{R(B_{11}^2-A_{11}D_{11})} \quad A_{s0710}=0$$

$$A_{s0801}=\left(\frac{A_{12}^2D_{11}+A_{11}B_{12}^2-2A_{12}B_{11}B_{12}}{B_{11}^2-A_{11}D_{11}}+A_{22}\right)\frac{\sin\alpha\cos\alpha}{R^2}$$

$$A_{s0802}=\left[(\frac{A_{12}^2D_{11}+A_{11}B_{12}^2-2A_{12}B_{11}B_{12}}{B_{11}^2-A_{11}D_{11}}+A_{22}+A_{44})\frac{n\cos\alpha}{R^2}+2I_0\cos\alpha(\Omega^2n-\Omega\omega)\right]$$

$$A_{s0803}=\left[\left(\frac{A_{12}^2D_{11}+A_{11}B_{12}^2-2A_{12}B_{11}B_{12}}{B_{11}^2-A_{11}D_{11}}+A_{22}\right)\frac{\cos^2\alpha}{R^2}+\frac{n^2A_{44}}{R^2}-I_0\omega^2+I_0\Omega^2n^2\right]$$

$$A_{s0804}=\left(\frac{A_{12}B_{12}D_{11}+A_{11}B_{12}D_{12}-A_{12}B_{11}D_{12}-B_{11}B_{12}^2}{B_{11}^2-A_{11}D_{11}}+B_{22}\right)\frac{\sin\alpha\cos\alpha}{R^2}$$

$$A_{s0805}=\left[\left(\frac{A_{12}B_{12}D_{11}+A_{11}B_{12}D_{12}-A_{12}B_{11}D_{12}-B_{11}B_{12}^2}{B_{11}^2-A_{11}D_{11}}+B_{22}\right)\frac{n\cos\alpha}{R^2}-A_{44}\frac{n}{R}+2I_1\cos\alpha(\Omega^2n-\Omega\omega)\right]$$

$$A_{s0806}=\frac{\cos\alpha(B_{11}B_{12}-A_{12}D_{11})}{R(B_{11}^2-A_{11}D_{11})}\quad A_{s0807}=0\quad A_{s0808}=-\frac{\sin\alpha}{R}\quad A_{s0809}=\frac{\cos\alpha(A_{12}B_{11}-A_{11}B_{12})}{R(B_{11}^2-A_{11}D_{11})}\quad A_{s0810}=0$$

$$A_{s0901}=\left[\left(\frac{A_{12}B_{12}D_{11}+A_{11}B_{12}D_{12}-A_{12}B_{11}D_{12}-B_{11}B_{12}^2}{B_{11}^2-A_{11}D_{11}}+B_{22}\right)\frac{\sin^2\alpha}{R^2}-I_1\omega^2+I_1\Omega^2n^2\right]$$

$$A_{s0902}=\left(\frac{A_{12}B_{12}D_{11}+A_{11}B_{12}D_{12}-A_{12}B_{11}D_{12}-B_{11}B_{12}^2}{B_{11}^2-A_{11}D_{11}}+B_{22}\right)\frac{n\sin\alpha}{R^2}+2I_1\sin\alpha(\Omega^2n-\Omega\omega)$$

$$A_{s0903}=\left(\frac{A_{12}B_{12}D_{11}+A_{11}B_{12}D_{12}-A_{12}B_{11}D_{12}-B_{11}B_{12}^2}{B_{11}^2-A_{11}D_{11}}+B_{22}\right)\frac{\sin\alpha\cos\alpha}{R^2}$$

$$A_{s0904}=\left[\left(\frac{B_{12}^2D_{11}+A_{11}D_{12}^2-2B_{11}B_{12}D_{12}}{B_{11}^2-A_{11}D_{11}}+D_{22}\right)\frac{\sin^2\alpha}{R^2}-I_2\omega^2+I_2\Omega^2n^2\right]$$

$$A_{s0905}=\left(\frac{B_{12}^2D_{11}+A_{11}D_{12}^2-2B_{11}B_{12}D_{12}}{B_{11}^2-A_{11}D_{11}}+D_{22}\right)\frac{n\sin\alpha}{R^2}+2I_2\sin\alpha(\Omega^2n-\Omega\omega)$$

$$A_{s0906}=\frac{\sin\alpha(B_{11}D_{12}-B_{12}D_{11})}{R(B_{11}^2-A_{11}D_{11})}\quad A_{s0907}=0\quad A_{s0908}=1\quad A_{s0909}=\left(\frac{B_{11}B_{12}-A_{11}D_{12}}{B_{11}^2-A_{11}D_{11}}-1\right)\frac{\sin\alpha}{R}\quad A_{s0910}=-\frac{n}{R}$$

$$A_{s1001}=\left(\frac{A_{12}B_{12}D_{11}+A_{11}B_{12}D_{12}-A_{12}B_{11}D_{12}-B_{11}B_{12}^2}{B_{11}^2-A_{11}D_{11}}+B_{22}\right)\frac{n\sin\alpha}{R^2}+2I_1\sin\alpha(\Omega^2 n-\Omega\omega)$$

$$A_{s1002}=\left[\left(\frac{A_{12}B_{12}D_{11}+A_{11}B_{12}D_{12}-A_{12}B_{11}D_{12}-B_{11}B_{12}^2}{B_{11}^2-A_{11}D_{11}}+B_{22}\right)\frac{n^2}{R^2}-A_{44}\frac{\cos\alpha}{R}-I_1\omega^2+I_1\Omega^2 n^2\right]$$

$$A_{s1003}=\left[\left(\frac{A_{12}B_{12}D_{11}+A_{11}B_{12}D_{12}-A_{12}B_{11}D_{12}-B_{11}B_{12}^2}{B_{11}^2-A_{11}D_{11}}+B_{22}\right)\frac{n\cos\alpha}{R^2}-\frac{nA_{44}}{R}+2I_1\cos\alpha(\Omega^2 n-\Omega\omega)\right]$$

$$A_{s1004}=\left(\frac{B_{12}^2D_{11}+A_{11}D_{12}^2-2B_{11}B_{12}D_{12}}{B_{11}^2-A_{11}D_{11}}+D_{22}\right)\frac{n\sin\alpha}{R^2}+2I_2\sin\alpha(\Omega^2 n-\Omega\omega)$$

$$A_{s1005}=\left[\left(\frac{B_{12}^2D_{11}+A_{11}D_{12}^2-2B_{11}B_{12}D_{12}}{B_{11}^2-A_{11}D_{11}}+D_{22}\right)\frac{n^2}{R^2}+A_{44}-I_2\omega^2+I_2\Omega^2 n^2\right]$$

$$A_{s1006}=\frac{n(B_{11}D_{12}-B_{12}D_{11})}{R(B_{11}^2-A_{11}D_{11})}\quad A_{s1007}=0\quad A_{s1008}=0\quad A_{s1009}=\frac{n(B_{11}B_{12}-A_{11}D_{12})}{R(B_{11}^2-A_{11}D_{11})}\quad A_{s1010}=-2\frac{\sin\alpha}{R}$$

$$[I_0,I_1,I_2]=\sum_{k=1}^{N_k}\int_{z_k}^{z_{k+1}}\rho[1,z,z^2]dz$$

Reference

[1] Afshari Hassan. 2020. “Effect of graphene nanoplatelet reinforcements on the dynamics of rotating truncated conical shells”, Journal of the Brazilian Society of Mechanical Sciences and Engineering Volume42, pp.1-22.

[2] Banerjee J.R., Ananthapuvirajah A. 2018. “Free vibration of functionally graded beams and frameworks using the dynamic stiffness method”, Journal of Sound and Vibration, Volume 422, pp.34-47.

[3] Dai Qiyi, Qin Zhaoye, Chu Fulei. 2021. “Parametric study of damping characteristics of rotating laminated composite cylindrical shells using Haar wavelets”, Thin–Walled Structures, Volume161, pp.107-112.

[4] El-Kaabazi Nihal, Kennedy David. 2012. “Calculation of natural frequencies and vibration modes of variable thickness cylindrical shells using the Wittrick–Williams algorithm”, Computers and Structures, Volume105, pp.4-12.

[5] Kwak Song Hun, Kim Kwang Hun, Yun Jong Guk, Kim Sok, Ri Phyong Chol. 2021. “Free vibration analysis of laminated closed conical, cylindrical shells and annular plates with a hole using a meshfree method”, Structures, Volume34, pp.3070-3086.

[6] Li Jun, Hua Hongxing. 2009. “Dynamic stiffness analysis of laminated composite beams using trigonometric shear deformation theory”, Composite Structures, Voume89, pp.433-442.

[7] Liu Xiang, Zhao Xueyi, Xie Chen. 2020. “Exact free vibration analysis for membrane assemblies with general classical boundary conditions”, Journal of Sound and Vibration, Volume485, pp.115-121.

[8] Liu Xiang, Sun Chengli, Ranjan Banerjee J., Dan Han-Cheng, Chang Le. 2021. “An exact dynamic stiffness method for multibody systems consisting of beams and rigid-bodies”, Mechanical Systems and Signal Processing, Volume150, pp.107-112.

[9] Shakouri M. 2019. “Free vibration analysis of

functionally graded rotating conical shells in thermal environment", Composites Part B, Volume163, pp.574-584.

[10] Su H., Banerjee J.R. 2015. "Development of dynamic stiffness method for free vibration of functionally graded Timoshenko beams", Computers and Structures, Volume147, pp.107-116.

[11] Thinh Tran Ich, Nguyen Manh Cuong. 2013. "Dynamic stiffness matrix of continuous element for vibration of thick cross-ply laminated composite cylindrical shells", Composite Structures, Volume98, pp.93-102.

[12] Tornabene Francesco, Fantuzzi Nicholas, Viola Erasmo, J.N. Reddy. 2014. "Winkler–Pasternak foundation effect on the static and dynamic analyses of laminated doubly-curved and degenerate shells and panels", Composites Part B, Volume57, pp.269-296.

[13] Ye Tiangui, Jin Guoyong, Chen Yuehua, Shi Shuangxia.2014. "A unified formulation for vibration analysis of open shells with arbitrary boundary conditions", International Journal of Mechanical Sciences, Volume81, pp.42-59.

[14]Zhang Chunyu, Ding Hu, Chen Hailong, Jin Guoyong, Ye Tiangui, Chen Yukun. 2018. "Dynamic modeling and characteristic analysis of the periodically coupled plate structure based on the dynamic stiffness method", Results in Physics, Volume11, pp.50-1160.